



Research Article

ISSN : 0975-7384  
CODEN(USA) : JCPRC5

## Fluid-Solid interaction modeling of cerebrospinal fluid absorption in arachnoid villi

M. Y. Abdollahzadeh Jamalabadi<sup>\*1,2</sup> and A. J. Keikha<sup>2</sup>

<sup>1</sup>Department of Mechanical, Robotics and Energy Engineering, Dongguk University, 30 Pildong-ro 1gil, Jung-gu, Seoul, Republic of Korea

<sup>2</sup>Chabahar Maritime University, Chabahar, Iran

### ABSTRACT

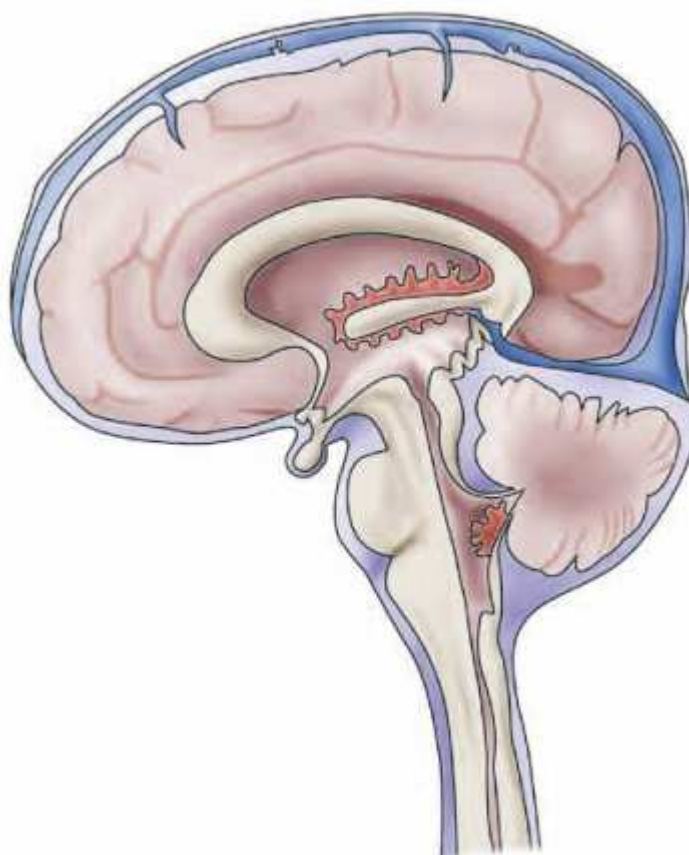
*As stated by the customary hypothesis, the cerebrospinal fluid (CSF) is secreted inside the brain ventricles and flows unidirectional along subarachnoid spaces to be absorbed into venous sinuses across arachnoid villi and via para-neural sheaths of nerves into lymphatics. Diffusion across the arachnoid granulations one-way valves into the superior sagittal sinus returns CSF to the venous circulation. Absorption of CSF into venous sinuses across arachnoid villi under the physiological pressure is considered here by means of considering fluid motion and solid response of arachnoid villi to them. A Fluid-Solid Interaction (FSI) model is constructed to simulate CSF flow. A comparison of the results and the experimental data was done. The previous rigid models have ignored the CFS interaction with arachnoid villi. In this computational fluid dynamic (CFD) analysis, the CSF pressure and flow velocity in different areas were concordant with the experimental data.*

**Keywords:** arachnoid villi; cerebrospinal fluid; Magnetic field; Fluid-Solid interaction

### INTRODUCTION

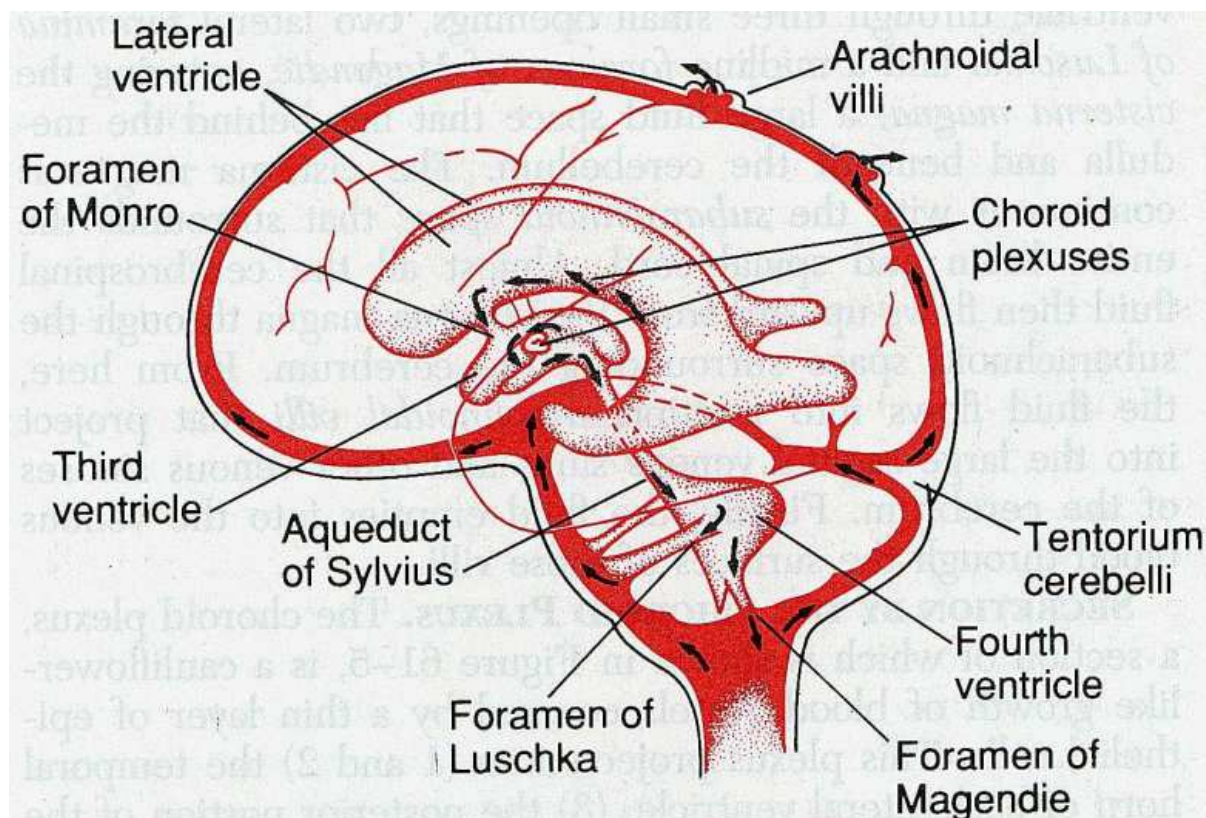
Cerebrospinal fluid (CSF) is considered a part of the transcellular fluids. It is contained in the ventricles and the subarachnoid space and bathes the brain and spinal cord. The CSF is contained within the meninges and acts as a cushion to protect the brain from injury with position or movement. It has been estimated that this cushioning or 'water bath' effect gives the 1400g brain an effective net weight of only 50g. CSF is a clear, colorless body fluid found in the brain and spine. It is produced in the choroid plexuses of the ventricles of the brain. It acts as a cushion or buffer for the brain's cortex, providing basic mechanical and immunological protection to the brain inside the skull. The CSF also serves a vital function in cerebral autoregulation of cerebral blood flow. The CSF occupies the subarachnoid space (between the arachnoid mater and the pia mater) and the ventricular system around and inside the brain and spinal cord. It constitutes the content of the ventricles, cisterns, and sulci of the brain, as well as the central canal of the spinal cord [1].

CSF circulates within the ventricular system of the brain. The ventricles are a series of cavities filled with CSF, inside the brain. The majority of CSF is produced from within the two lateral ventricles. From here, the CSF passes through the interventricular foramina to the third ventricle, then the cerebral aqueduct to the fourth ventricle. The fourth ventricle is an outpouching on the posterior part of the brainstem. From the fourth ventricle, the fluid passes through three openings to enter the subarachnoid space – these are the median aperture, and the lateral apertures. The subarachnoid space covers the brain and spinal cord. The CSF moves in a pulsatile manner throughout the CSF system with a nearly zero net flow [2].



**Fig. 1.**The cerebrospinal fluid (CSF) circulates in the subarachnoid space around the brain and spinal cord

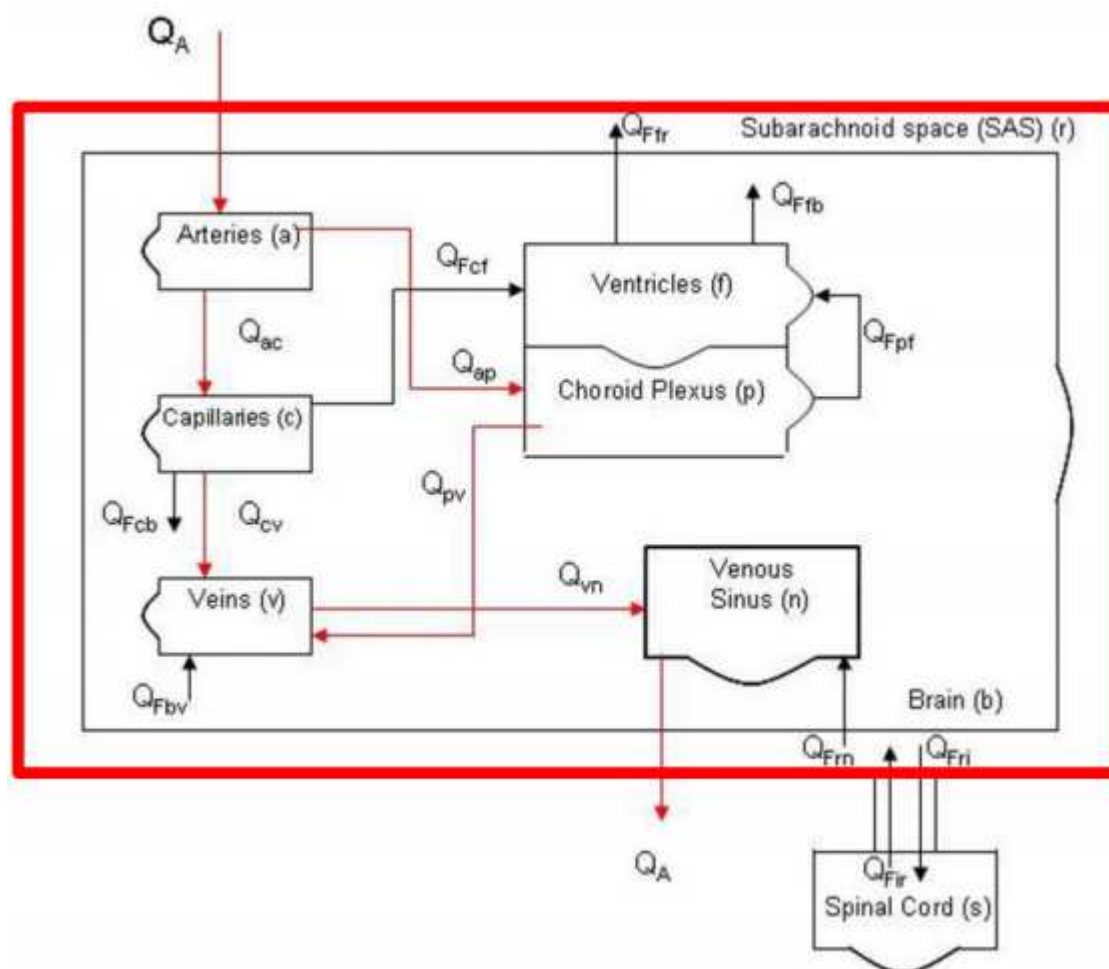
CSF serves several purposes as buoyancy, protection, chemical stability, prevention of brain ischemia, and clearing waste. The actual mass of the human brain is about 1400 grams; however, the net weight of the brain suspended in the CSF is equivalent to a mass of 25 grams. The brain therefore exists in neutral buoyancy, which allows the brain to maintain its density without being impaired by its own weight, which would cut off blood supply and kill neurons in the lower sections without CSF. CSF protects the brain tissue from injury when jolted or hit. In certain situations such as motor vehicle crashes or sports injuries, the CSF cannot protect the brain from forced contact with the skull case, causing hemorrhaging, brain damage, and sometimes death. CSF flows throughout the inner ventricular system in the brain and is absorbed back into the bloodstream, rinsing the metabolic waste from the central nervous system through the blood–brain barrier. This allows for homeostatic regulation of the distribution of neuroendocrine factors, to which slight changes can cause problems or damage to the nervous system. For example, high glycine concentration disrupts temperature and blood pressure control, and high CSF pH causes dizziness and syncope. To use Davson's term, the CSF has a "sink action" by which the various substances formed in the nervous tissue during its metabolic activity diffuse rapidly into the CSF and are thus removed into the bloodstream as CSF is absorbed. The prevention of brain ischemia is made by decreasing the amount of CSF in the limited space inside the skull. This decreases total intracranial pressure and facilitates blood perfusion. CSF has been shown by the research group of Maiken Nedergaard to be critical in the brain's glymphatic system, which plays an important role in flushing metabolic toxins or waste from the brain's tissues' cellular interstitial fluid (ISF). CSF flushing of wastes from brain tissue is further increased during sleep, which results from the opening of extracellular channels controlled through the contraction of glial cells, which allows for the rapid influx of CSF into the brain. These findings indicate that CSF may play a large role during sleep in clearing metabolic waste, like beta amyloid, that are produced by the activity in the awake brain [3].



**Fig. 2.** Anatomy of cranial CSF spaces (Volume of brain= 1400 ml; Volume of CSF= 150ml; CSF in ventricles around 25 ml; Volume of blood= 150 ml; Total volume of cerebrospinal fluid (adult) = 125-150 ml (infant) = 50 ml; Turnover of entire volume of cerebrospinal fluid = 3 to 4 times per day; Rate of production of CSF = 0.35 ml/min (500 ml/day); pH of cerebrospinal fluid = 7.33) [from Kandel et al., 2000, p. 1296]

The total volume of CSF is 150 mls. The daily production is 550 mls/day so the CSF turns over about 3 to 4 times per day. The CSF is formed by the choroid plexus (50%) and directly from the walls of the ventricles (50%). CSF flows through the foramina of Magendie & Luschka into the subarachnoid space of the brain and spinal cord. It is absorbed by the arachnoid villi (90%) and directly into cerebral venules (10%). The normal intracerebral pressure (ICP) is 5 to 15 mmHg. The rate of formation of CSF is constant and is not affected by ICP. Absorption of CSF increases linearly as pressure rises above about 7 cmsH<sub>2</sub>O pressure. At a pressure of about 11cmsH<sub>2</sub>O, the rate of secretion & absorption are equal. The CSF has a composition identical to that of the brain ECF but this is different from plasma. The major differences from plasma are:

- The pCO<sub>2</sub> is higher (50 mmHg) resulting in a lower CSF pH (7.33)
- The protein content is normally very low (0.2g/l) resulting in a low buffering capacity
- The glucose concentration is lower
- The chloride concentration is higher
- The cholesterol content is very low

Fig. 3. circulation and volumes in SAS ( $V_{brain} + V_{blood} + V_{csf} = \text{const}$ )

There are no lymphatic channels in the brain and CSF fulfils the role of returning interstitial fluid and protein to the circulation. The CSF is separated from blood by the blood-brain barrier. Only lipid soluble substances can easily cross this barrier and this is important in maintaining the compositional differences.

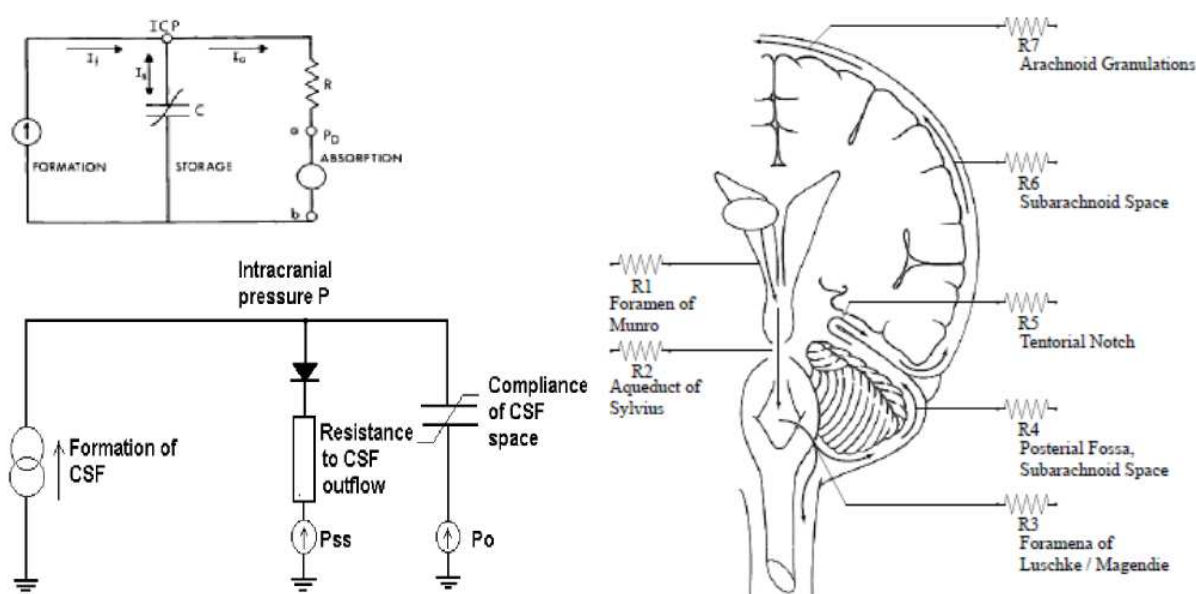


Fig. 4. Electrical model of CSF circulation and pressure- volume Compensation and Components of resistance to CSF outflow



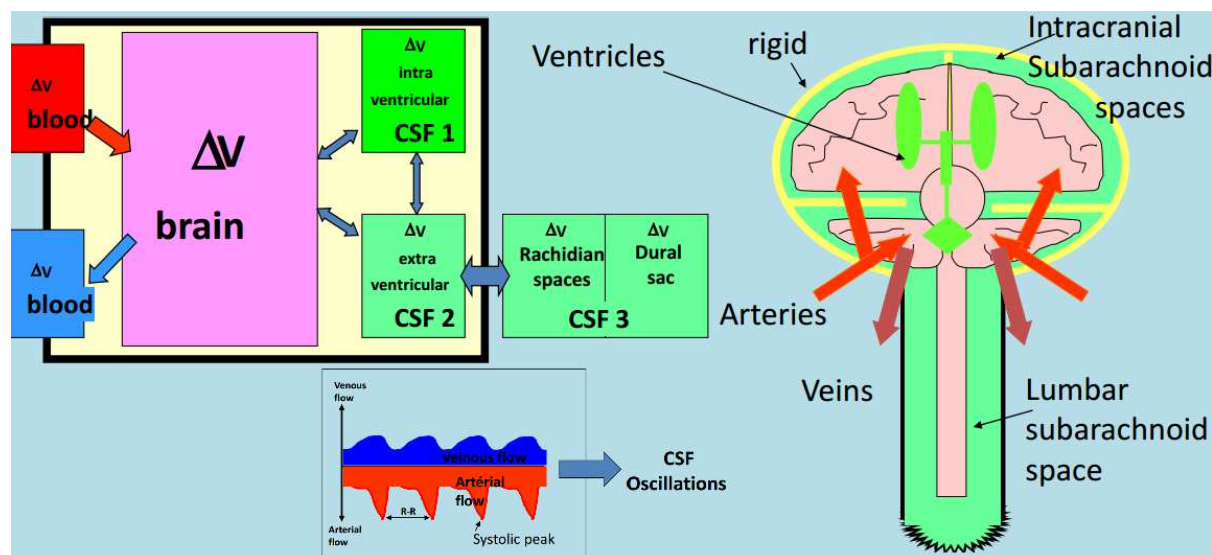


Fig. 5.pulsatile CSF flow (Aqueductal CSF Velocity= 10 cm/sec ; Cervical blood Velocity=80 cm/sec; Cervical CSF Velocity = 5 cm/sec)

### EXPERIMENTAL SECTION

The cerebrospinal fluid (CSF) is produced from arterial blood by the choroid plexuses of the lateral and fourth ventricles by a combined process of diffusion, pinocytosis and active transfer. A small amount is also produced by ependymal cells. The choroid plexus consists of tufts of capillaries with thin fenestrated endothelial cells. These are covered by modified ependymal cells with bulbous microvilli. The total volume of CSF in the adult ranges from 140 to 270 ml. The volume of the ventricles is about 25 ml. CSF is produced at a rate of 0.2 - 0.7 ml per minute or 600-700 ml per day. The circulation of CSF is aided by the pulsations of the choroid plexus and by the motion of the cilia of ependymal cells. CSF is absorbed across the arachnoid villi into the venous circulation and a significant amount probably also drains into lymphatic vessels around the cranial cavity and spinal canal. The arachnoid villi act as one-way valves between the subarachnoid space and the dural sinuses. The rate of absorption correlates with the CSF pressure. CSF acts as a cushion that protects the brain from shocks and supports the venous sinuses (primarily the superior sagittal sinus, opening when CSF pressure exceeds venous pressure). It also plays an important role in the homeostasis and metabolism of the central nervous system. CSF from the lumbar region contains 15 to 45 mg/dl protein (lower in children) and 50-80 mg/dl glucose (two-thirds of blood glucose). Protein concentration in cisternal and ventricular CSF is lower. Normal CSF contains 0-5 mononuclear cells. The CSF pressure, measured at lumbar puncture (LP), is 100-180 mm of H<sub>2</sub>O (8-15 mm Hg) with the patient lying on the side and 200-300 mm with the patient sitting up.

The brain produces roughly 500 mL of cerebrospinal fluid per day. This fluid is constantly reabsorbed, so that only 100-160 mL is present at any one time. Ependymal cells of the choroid plexus produce more than two thirds of CSF. The choroid plexus is a venous plexus contained within the four ventricles of the brain, hollow structures inside the brain filled with CSF. The remainder of the CSF is produced by the surfaces of the ventricles and by the lining surrounding the subarachnoid space[1].

Ependymal cells actively secrete sodium into the lateral ventricles. This creates osmotic pressure and draws water into the CSF space. Chloride, with a negative charge, moves with the positively charged sodium and a neutral charge is maintained. As a result, CSF contains a higher concentration of sodium and chloride than blood plasma, but less potassium, calcium and glucose and protein [1-2].



**Fig. 6.** Vials containing human cerebrospinal fluid

It had been thought that CSF returns to the vascular system by entering the Dural venous sinuses via the arachnoid granulations (or villi). However, some [3] have suggested that CSF flow along the cranial nerves and spinal nerve roots allow it into the lymphatic channels; this flow may play a substantial role in CSF reabsorption, in particular in the neonate, in which arachnoid granulations are sparsely distributed. The flow of CSF to the nasal submucosal lymphatic channels through the cribriform plate seems to be especially important [4]. The CSF is created from blood plasma and is largely similar to it, except that CSF is nearly protein-free compared with plasma and has some modified electrolyte levels. CSF contains approximately 0.3% plasma proteins, or approximately 15 to 40 mg/dL, depending on sampling site [5] and it is produced at a rate of 500 ml/day. Since the subarachnoid space around the brain and spinal cord can contain only 135 to 150 ml, large amounts are drained primarily into the blood through arachnoid granulations in the superior sagittal sinus. Thus the CSF turns over about 3.7 times a day. This continuous flow into the venous system dilutes the concentration of larger, lipid-insoluble molecules penetrating the brain and CSF [6]. Healthy cerebrospinal fluid is free of red blood cells, and at most contains only a few white blood cells. Any cell count higher than that constitutes pleocytosis, an excess of cells. CSF pressure, as measured by lumbar puncture (LP), is 10-18 cmH<sub>2</sub>O (8-15 mmHg or 1.1-2 kPa) with the patient lying on the side and 20-30 cmH<sub>2</sub>O (16-24 mmHg or 2.1-3.2 kPa) with the patient sitting up [8]. In newborns, CSF pressure ranges from 8 to 10 cmH<sub>2</sub>O (4.4-7.3 mmHg or 0.78-0.98 kPa). Most variations are due to coughing or internal compression of jugular veins in the neck. When lying down, the cerebrospinal fluid as estimated by lumbar puncture is similar to the intracranial pressure.

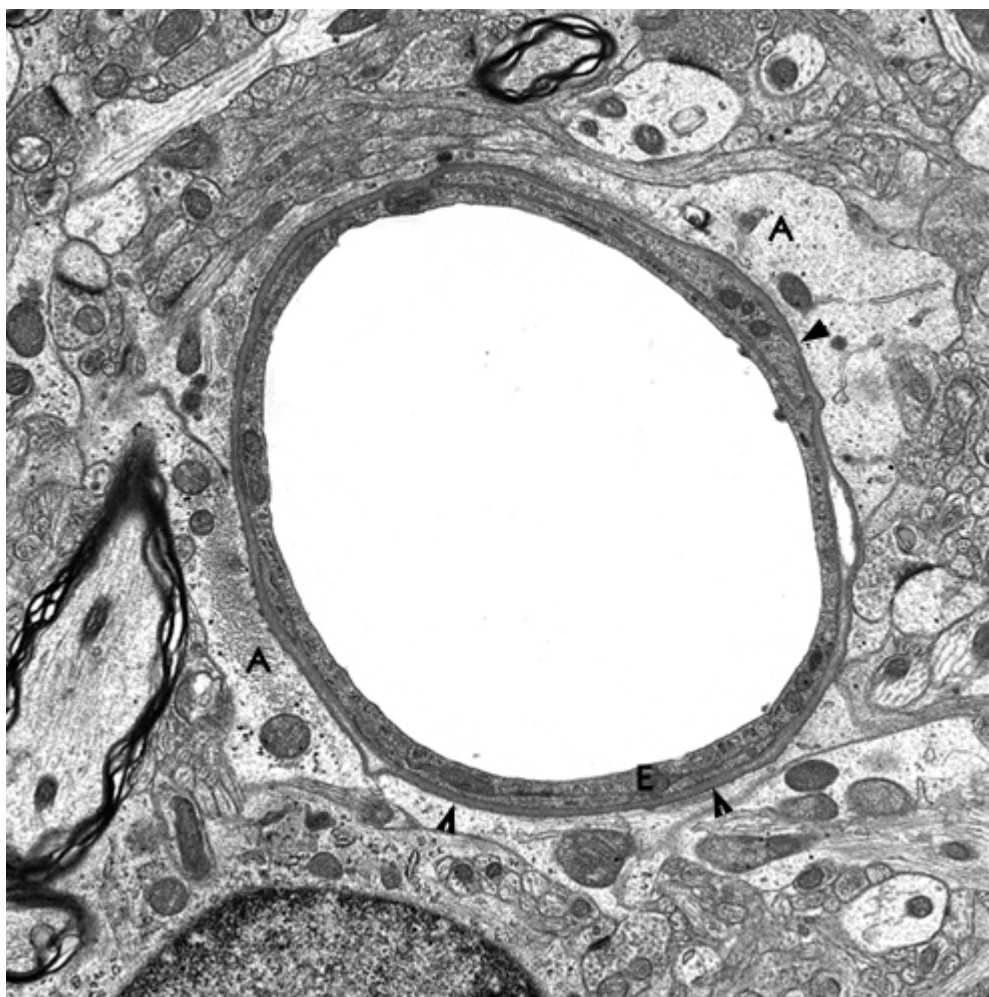


**Fig. 7.**Brain capillary. A:astrocytic processes; E:endothelium; Arrow heads: vasular basement membrane

Unlike other organs and tissues, the endothelial cells that line brain capillaries have no fenestrations or pinocytotic (transportation) vesicles and have tight and adherens junctions that almost fuse adjacent endothelial cells. Moreover, these endothelial cells have different receptors and ion channels on their surface than on the surfaces facing the brain, an arrangement that facilitates transcellular transport. This anatomy is the basis of the blood-brain barrier (BBB). The endothelial cells are surrounded by a discontinuous layer of pericytes, and these vascular cells are enclosed within a basement membrane made up of collagens, laminins, and proteoglycans. Astrocytic processes cover the capillaries, and perivascular macrophages are interposed between them and the capillary basement membrane. During development, astrocytes induce brain endothelial cells to develop in this special leak-proof fashion. The BBB separates plasma from the interstitial space of the CNS and is key to maintaining homeostasis in the CNS. It controls the traffic of molecules, including ions and water in and out of the brain and plays an important role in supplying the brain with nutrients and getting rid of waste and toxic products. The ability to exclude certain substances from brain interstitial space has to do not only with the vascular anatomy, but also with lipid solubility and selective transcellular transport by endothelial cells. Lipophilic compounds cross the BBB easier than hydrophilic ones do, and small lipophilic molecules such as O<sub>2</sub> and CO<sub>2</sub> diffuse freely. Hydrophilic substances can only get across brain capillaries through endothelial cells rather than between them. Some hydrophilic molecules, including glucose and amino acids, enter endothelial cells with the help of transporters, and larger molecules, including proteins, enter via receptor-mediated endocytosis and exit along the opposite surface by exocytosis. GLUT1 is the glucose transporter. The ATP-binding cassette (ABC) transporters are important for transport of lipophilic substances and efflux of toxic metabolites. The BBB protects the brain from toxic substances but also impedes the entry of drugs. Circulating leukocytes enter the brain by passing through endothelial cells rather than between them. Astrocytes cover almost the entire surface of brain capillaries; they are interposed between the vasculature and neurons thus linking neuronal activity to BBB function. Hypertonic stimuli and chemical substances including glutamate and certain cytokines can open the BBB.

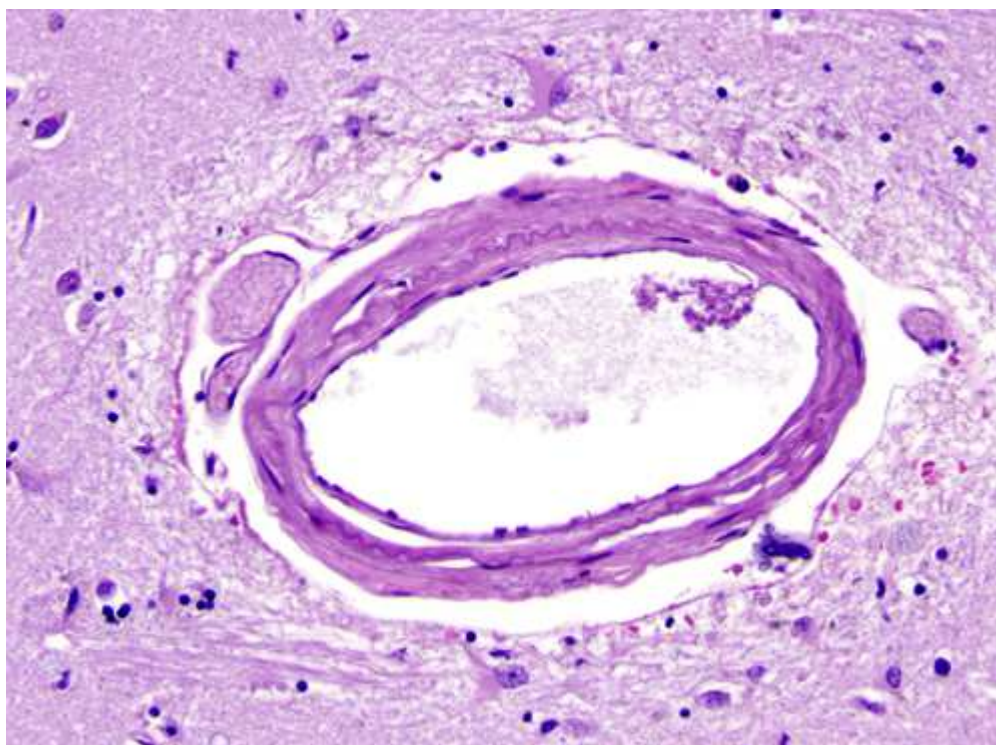


Fig. 8. Perivascular (Virchow-Robin) space around a small artery. The VRS is exaggerated in paraffin-processed specimens

The outer surface of this perivascular space (PVS) is formed by the glia limitans. The inner surface is the vascular basement membrane. Postcapillary venules are also surrounded by a PVS. The PVS that surrounds postcapillary venules is the portal of entry of leukocytes into the brain in the normal state and during inflammation. Circulating monocytes and lymphocytes normally traverse postcapillary venules and enter the PVS. In the course of inflammation, such as MS, this entry is increased because of leukocyte interactions with inflamed endothelial cells. Furthermore, leukocytes penetrate the glia limitans and enter into the CNS. The latter move is facilitated by matrix metalloproteinases (MMPs) produced by macrophages, which loosen the glia limitans.

Table 1. Characteristics of CSF

Substance	Cerebrospinal Fluid
Water Content (%)	99
Protein (mg/dL)	35
Glucose (mg/dL)	60
Osmolarity (mOsm/L)	295
Sodium (mEq/L)	138
Potassium (mEq/L)	2.8
Calcium (mEq/L)	2.1
Magnesium (mEq/L)	0.3
Chloride (mEq/L)	119
pH	7.33

The main equations for CSF-flow are provided in vector type by equations (1) and (2) as shown below. The governing equations are:

$$\text{div } \bar{V} = 0 \quad (1)$$

$$\rho \frac{d\bar{V}}{dt} = \text{div } \bar{T} \quad (2)$$

where  $\frac{d}{dt}$  is the material derivative,  $\bar{V}$  is the velocity,  $\rho$  is the density,  $C$  is the specific heat,  $J$  is the current density,  $\mathbf{q}_r$  is the radiative heat,  $B$  is the total magnetic field (the induced magnetic field assumed negligible),  $T$  is temperature, and  $\bar{T}$  is the Cauchy stress tensor. The constitutive equation for  $\bar{T}$  in a third order fluid is

$$\bar{T} = -p\bar{I} + \bar{S} \quad (3)$$

where  $p$  is the pressure,  $I$  is the identity tensor and the extra stress tensor  $S$  is given by



$$\bar{S} = \mu \bar{A}_1 + \alpha_1 \bar{A}_2 + \alpha_2 \bar{A}_1^2 + \beta_1 \bar{A}_3 + \beta_2 (\bar{A}_2 \bar{A}_1 + \bar{A}_1 \bar{A}_2) + \beta_3 (tr \bar{A}_1^2) \bar{A}_1 \quad (4)$$

In the FSI model, brain parenchyma is modeled like a linear elastic substance in contact with CSF fluid and for mathematical modeling the Arbitrary-Lagrangian Eulerian (abbreviated as ALE) formulation is applied to be like the prevailing rule.

## RESULTS AND DISCUSSION

This section introduces the results of the computer predictions for the interactions of all cerebral compartments. The emphasis lies on comparing the differences between normal and hydrocephalic cases to highlight pathological changes and offer to mechanistic explanations. In both the rigid and the FSI models, the stream is implicit to be laminar, along with CSF is considered Newtonian, viscous and incompressible. The conservation balances result to a structure of biased differential equations referred to as continuity as well as the Navier-Stokes equations. The inflow is the CSF production from choroid plexus lateral ventricle and the third ventricles. The outflow is from the Luschka and Magendie foramina and considered to have zero pressure to obtain the pressure distribution. The immense production is as a result of CSF production in the choroid plexus which is a pulsatile generation due to the arterioles pulsation in choroid plexus synchronized with the heartbeat. The rate of recurrence of the pulsatile movement is put to 1 Hz (approximating kin to the usual cardiac cycle). For simplification, we considered a relative pressure (zero value) at the end of Magendie foramina.

The outcomes of the CSF-analysis are the flow-rate, velocities, as well as ICP-gradients of CSF in the ventricular-system. In addition, obtaining the lateral ventricular displacement and stress distribution in solid part are the parameters which were calculated in the deformable model. Our study not only considered rigid boundary condition but also the surrounding flexible brain tissue interaction effect with pulsatile inflow. The previous simulation results were based on rigid boundary condition for the walls of ventricles. Linninger (Ursino, 1988) modeled the brain effects as a rigid porous media. His investigation showed the necessity of considering surrounding tissue interaction with CSF flow pattern. The brain tissue is a solid material and in some research works has been modeled as an elastic material (Balédent et al., 2004). Also, Fin compared the rigid and deformable models for aqueduct. However, his model considered a solid thickness for the aqueduct wall instead of whole parenchyma interaction without considering the pulsatile in flow. In later publications, Cheng et al. (Yoo et al., 2012) considered the effect of parenchyma as an elastic membrane with different elastic properties and different portions and applying the arbitrary load and reproducing the pulsatile nature of CSF flow. Though 2D models provide a quantitative simulation of CSF flow in the ventricles, the qualitative results provided through such models are more reliable. A more realistic 3D model of HVS geometry though seems to yield more accurate results, is a complex and cumbersome task which has not been seen in recent literature. We propose that CSF flow and interaction of the parenchyma to be modeled in a 3D pattern for future studies. Another shortcoming in our modeling is that the brain parenchyma is treated as an elastic material, causing the ventricular walls to return to their previous position after each pulsation. However, as the work of Miller and coworkers (Yoo et al., 2012) has shown, the mechanical behavior of the brain tissue is more appropriately explained with visco-elastic or non-linear hyper elastic models. Another probable pitfall in our 2D model is that the SAS chamber and diffusion of CSF into the venous sinuses has not been considered, which does not seem to be a major obstacle considering the recent advances in CFD software package. Efforts are underway to extend the model presented here in to a 3D model of brain ventricle, SAS and parenchyma, capable of describing the absolute pressure in HVS system. Also we have not considered brain arterial pulsations in our model. The effect of this can be considered for future study.

**Table 2. Material properties for the bi-phasic model of intracranial dynamics**

Location	property	Value
Brain parenchyma	Porosity, $\phi$	0.3 (Lakin et al. 2003)
Brain parenchyma	Permeability, $k_{\text{exf}}$ ( $\text{m}^2$ )	$0.7 \times 10^{-15}$ (Lakin et al. 2003)
Brain parenchyma	Density, $\rho$ ( $\text{kg}/\text{m}^3$ )	1050 (Pellicer et al. 2006)
Brain parenchyma	Viscosity, $\mu$ ( $\text{kg}/\text{mper s}$ )	0.001
Venous flow	Max/min ( $\text{ml}/\text{min}$ )	882/630 (Kim et al. 2007)
Blood	density, $\rho$ ( $\text{kg}/\text{m}^3$ )	1050 (Pedley 1980)
Blood	Viscosity, $\mu$ ( $\text{kg}/\text{mper s}$ )	0.004 (Pedley 1980)
CSF	Density, $\rho_{\text{CSF}}$ ( $\text{kg}/\text{m}^3$ )	998.2 (Lakin et al. 2003)
CSF	Viscosity, $\mu$ ( $\text{kg}/\text{mper s}$ )	0.001
Phase lag	% Cardiac cycle Predicted	13%/12% in (Kim et al. 2007)
Cerebral blood flow	Mean ( $\text{ml}/\text{min}$ )	738

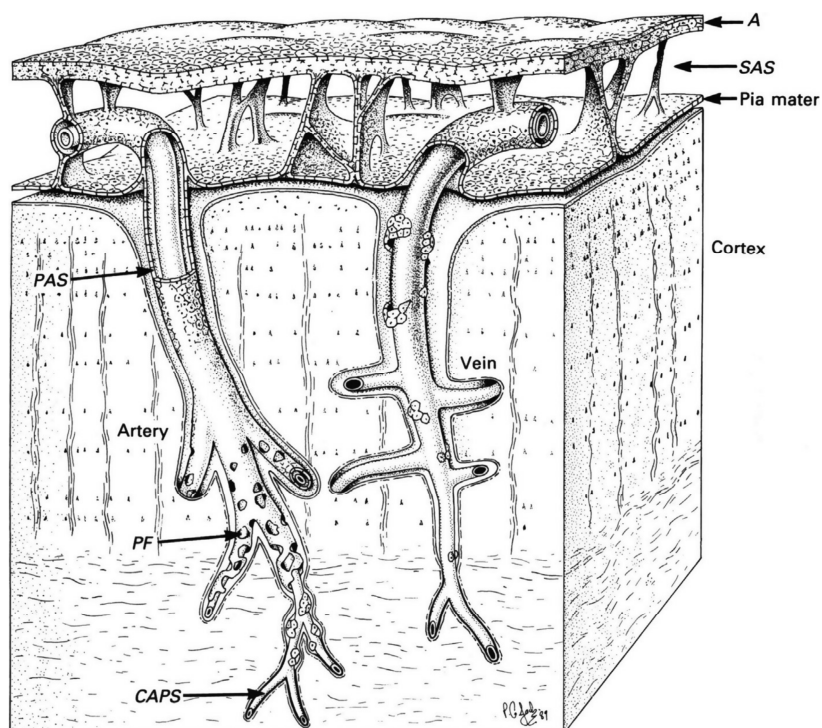


Fig. 9. Real schematic of problem

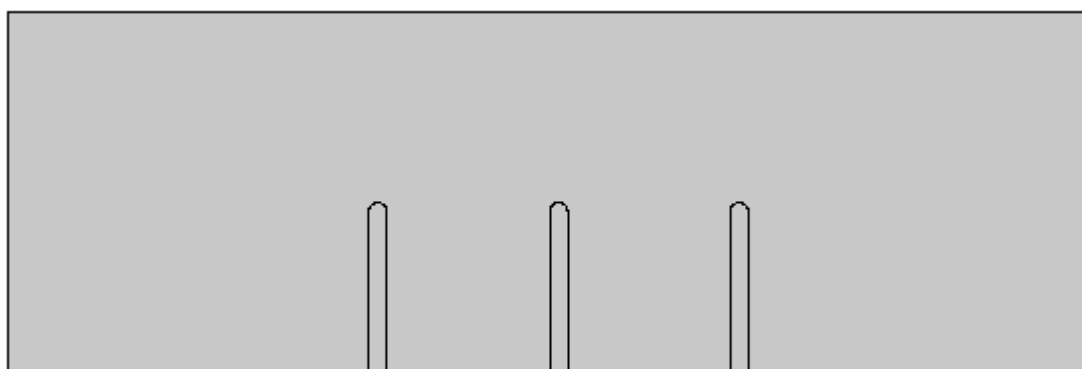


Fig. 10. Computational schematic of problem

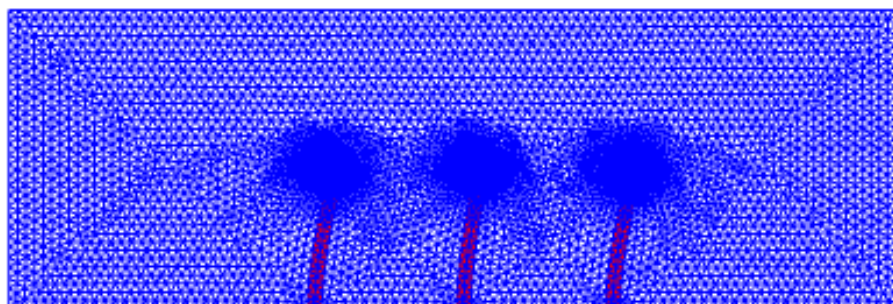
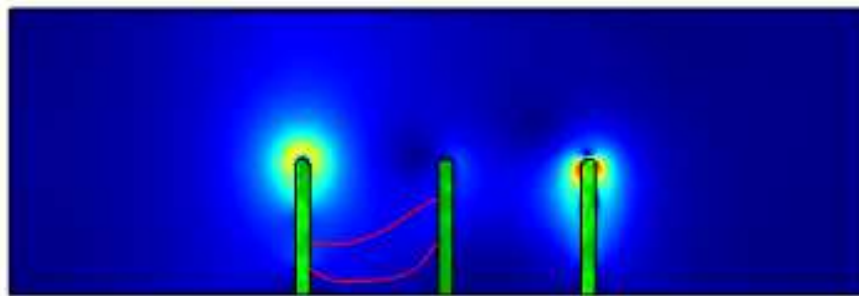
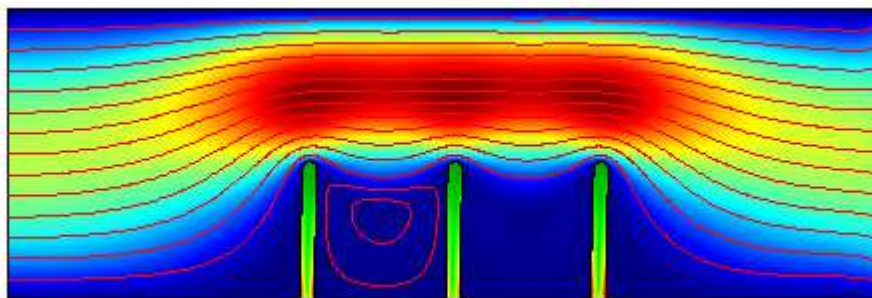
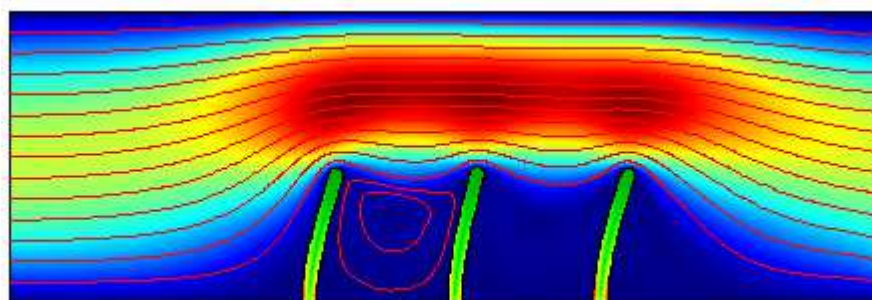
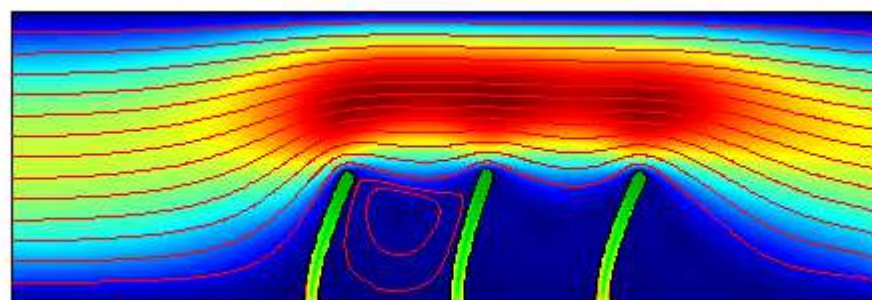
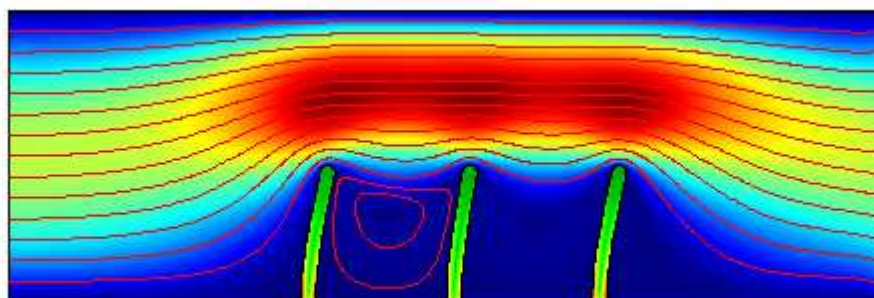
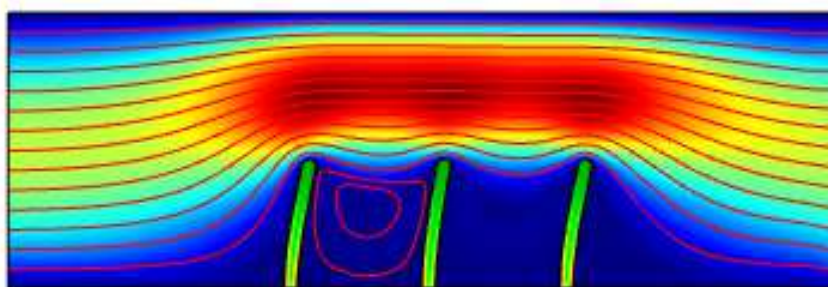
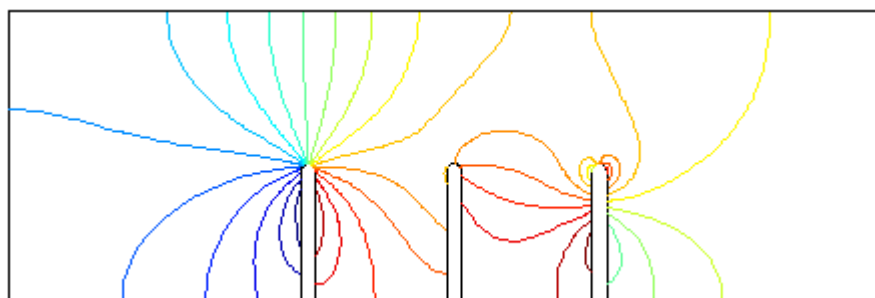
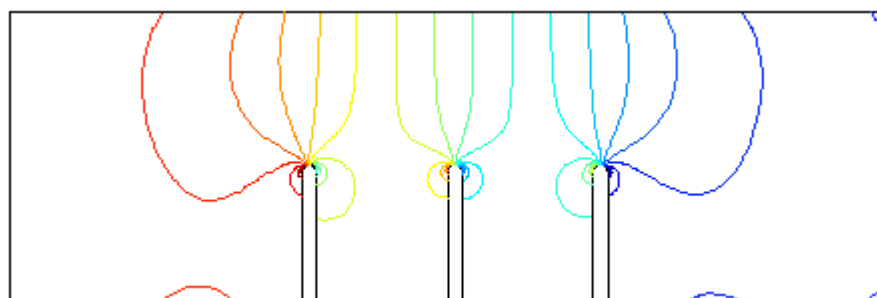
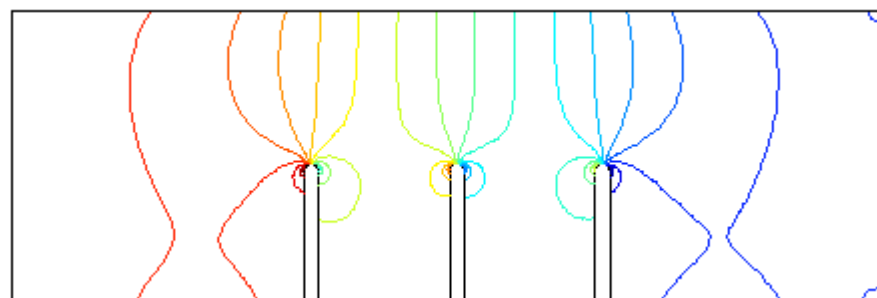
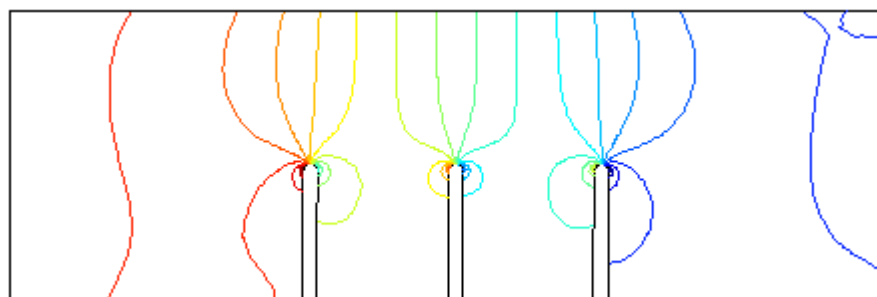
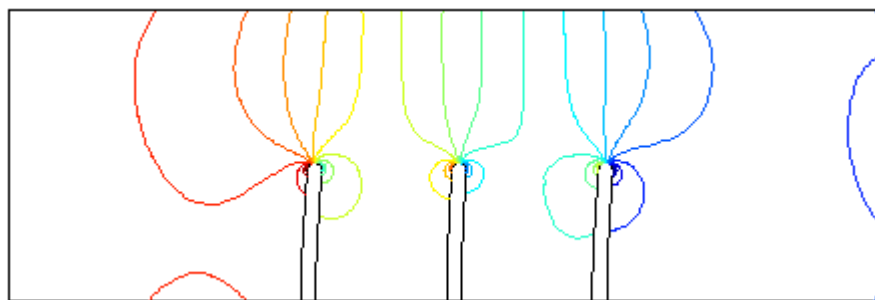
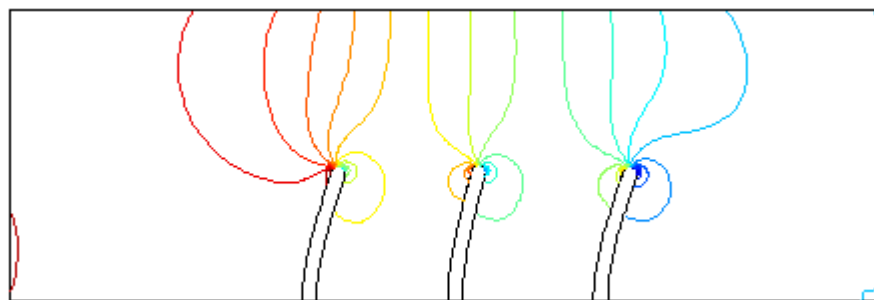
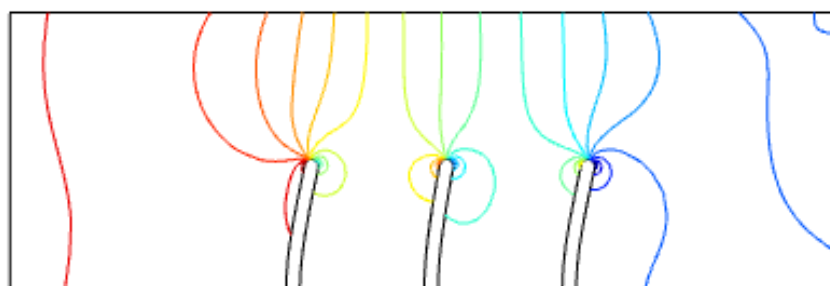


Fig. 11. Moving mesh for problem

Fig. 12. Velocity magnitude contour and streamline at  $t=0.001$  (s)Fig. 13. Velocity magnitude contour and streamline at  $t=0.07$  (s)Fig. 14. Velocity magnitude contour and streamline at  $t=0.17$  (s)Fig. 15. Velocity magnitude contour and streamline at  $t=0.17$  (s)Fig. 16. Velocity magnitude contour and streamline at  $t=0.17$  (s)

Fig. 17.Velocity magnitude contour and streamline at  $t=4$  (s)Fig. 18.Pressure field at  $t=0.001$  (s)Fig. 19.Pressure field at  $t=0.005$  (s)Fig. 20.Pressure field at  $t=0.01$  (s)Fig. 21.Pressure field at  $t=0.05$  (s)



Fig. 22. Pressure field at  $t = 0.1$  (s)Fig. 23. Pressure field at  $t = 0.2$  (s)Fig. 24. Pressure field at  $t = 0.3$  (s)Fig. 25. Pressure field at  $t = 4$  (s)

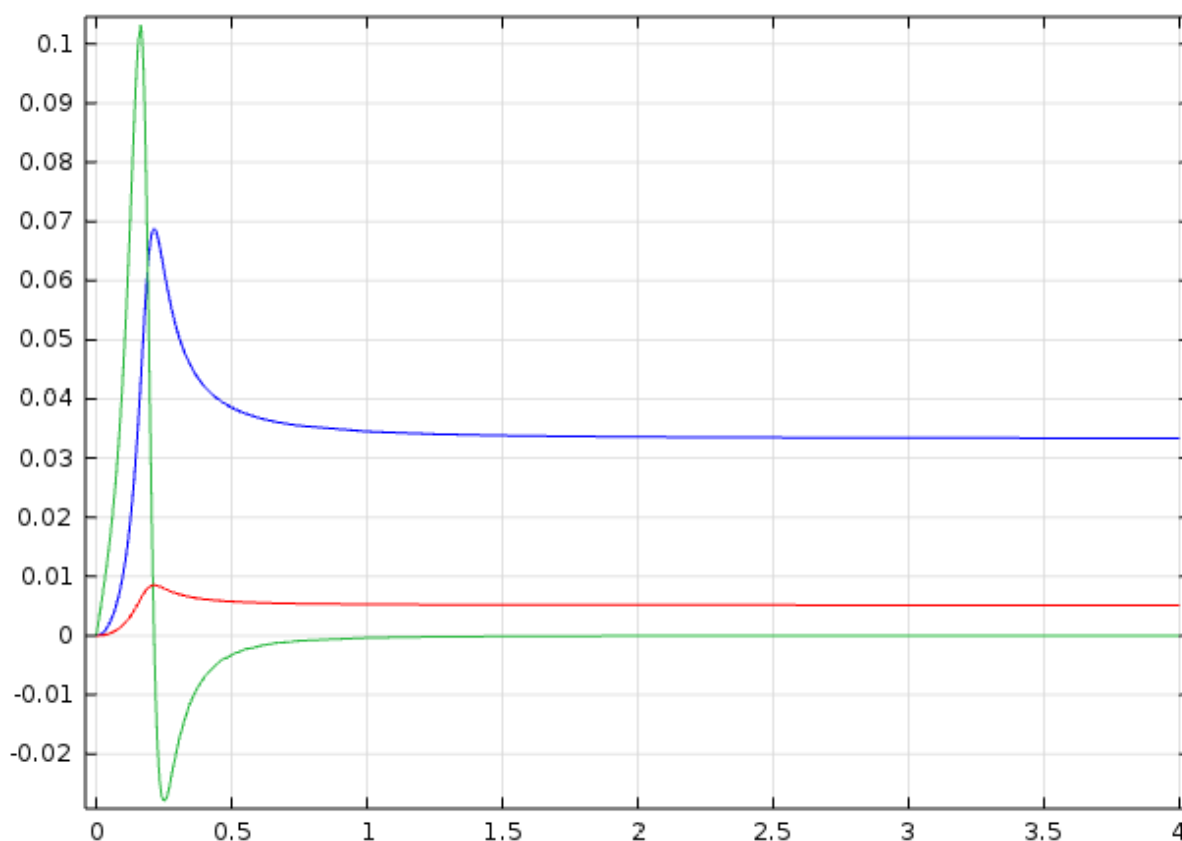


Fig. 26. Villi responses to pressure changes of main blood flow

We have developed a model for intracranial dynamics in which the interactions of all compartments are quantified by fundamental mass and force conservation balances. Under normal conditions, CSF motion is produced by the vascular expansion and pulsatile brain deformation. Since the parenchyma is incompressible, its deformation is passed on to the ventricles, forcing CSF displacement from the confined cranium into the spinal canal. The Monro-Kellie doctrine is fully satisfied in our model and we have predicted a CSF displacement into the spinal canal of about 0.9 ml in each cardiac cycle. For normal dynamics, the pulsations of the lateral ventricles as well as the amplitudes and pressure gradients of arteries, arterioles, capillaries, venules and veins can be calculated. It is important to recognize that in simulating communicating hydrocephalus we have simplified the situation for analysis. Firstly, the model does not divide the cerebral subarachnoid space into compartments. Quite likely some forms of hydrocephalus are caused by adsorption blocks at the arachnoid granulations and others by more proximal blocks at the base of the brain. These two situations cannot be distinguished in the current state of the model so the volume changes and pressure in the single cerebral subarachnoid space may be different from what actually occurs. The model, as it stands, predicts that the cerebral subarachnoid space is slightly increased with hydrocephalus. Clinical MRI observations, on the other hand, show a decrease in subarachnoid space in communicating hydrocephalus. MRI measurements need to be quantified in cases of acute hydrocephalus, and our model needs further spatial development to account for changes of the parenchymal cell matrix.

## CONCLUSION

In this letter, we derived and analyzed a mathematical model subject to low Reynolds number approximations in order to study the motion of CS fluid and the impacts of villi solid in a horizontal tube. Analysis has been carried out in the presence of arachnoid villi absorptions sites. Exact expressions for velocity field and averaged flow rate are obtained. The results extracted are compatible with the physical expectations and are found to satisfy all the subjected conditions. A side by side comparative analysis is performed to compare our findings between theory and experiments. Moreover, CF fluid model reduces a classical Navier Stokes fluid model can be deduced from this as a special case. This provides a useful accuracy check about the correctness and validity of our results and provides a strong confidence into the presented mathematical descriptions.

## REFERENCES

- [1] MY AbdollahzadehJamalabadi, *J Porous Media*, **2015**, 18( 9) ,843-860.
- [2] MY AbdollahzadehJamalabadi, *Int J Opt Appl*, **2015**, 5 (5) , 161-167
- [3] MY AbdollahzadehJamalabadi, *ChemEng Res Des*, **2015**, 102 , 407-415
- [4]MY AbdollahzadehJamalabadi; JH Park ; CY Lee, *entropy*, **2015**, 17 (2), 866-881
- [5] Martini, Timmons, Tallitsch, Frederick, Michael, Robert ,**2015**, Human Anatomy (Eighth ed.). Boston: Pearson. p. 453.
- [6] L. F. Edwards ,**1934**, Anatomy for physical education, descriptive and applied.
- [7] H. Morris ,**1921**, Morris's human anatomy.
- [8] Sampson, J.H., Brady, M.L., Petry, N.A., Croteau, D., Friedman, A.H., Friedman, H.S., Wong, T., Bigner, D.D., Pastan, I., Puri, R.K., and Pedain, C., **2007**, *Neurosurgery*, 60(2),89-98.
- [9] Roberts, T.P.L., **1997**, *J. Magn. Reson. Imaging*, 7(1), 82-90.
- [10] Strich, G., Hagan, P.L., Gerber, K.H., and Slutsky, R.A., **1985**, *Radiology*,154(3), 723-726.
- [11] Stanisiz, G.J. and Henkelman, R.M., **2000**, *Magn. Reson. Med.*, 44(5), 665-667.
- [12] Gurbanova, A.A., Aker, R., Berkman, K., Onat, F.Y., van Rijn, C.M., and van Luijteleaar, G., **2006**, *Br. J. Pharmacol.*, 148(8), 1076-1082.
- [13] Sarntinoranont, M., Banerjee, R.K., Lonser, R.R., and Morrison, P.F., **2003**, *Ann. Biomed. Eng.*, 31(4), 448-461.
- [14] McGuire, S., Zaharoff, D., and Yuan, F., **2006**, *Ann. Biomed. Eng.*, 34(7), 1173-1181.
- [15] Sarntinoranont, M., Chen, X.M., Zhao, J.B., and Mareci, T.H., **2006**, *Ann. Biomed. Eng.*, 34(8), 1304-1321.
- [16] Chen, X.M., Dunn, A.C., Sawyer, W.G., and Sarntinoranont, M., **2007**, *J. Biomech. Eng.-Trans.ASME*, 129(2), 156-163.
- [17] Nicolson, P.C. and Vogt, J., **2001**, *Biomaterials*, 22, 3273-3283.
- [18] Yang, W.-H., Smolen, V.F., and Peppas, N.A., **1981**, *J. Membrane Sci.*, 9, 53-67.
- [19] Jones, L.W. and Jones, D.A., **2000**, Butterworth-Heinemann.
- [20] Holden, B.A., Stephenson, A., Stretton, S., Sankaridurg, P.R., O'Hare, N., Jalbert, I., and Sweeney, D.F., **2001**, *Optometry and Vision Science*, 78(1), 9-12.
- [21] Kikkawa, Y., Soft Contact Lens Kinetics, in Contact Lens Practice, Ruben, M. and Guillon, M., Editors. **1994**, Chapman & Hall. p. 113-121.
- [22] Hinkley, J.A., Morgret, L.D., and Gehrke, S.H., **2004**, *Polymer*, 45(26), 8837-8843.
- [23] Drury, J.L., Dennis, R.G., and Mooney, D.J., **2004**, *Biomaterials*, 25(16), 3187-3199.
- [24] Stammen, J.A., Williams, S., Ku, D.N., and Guldberg, R.E., **2001**, *Biomaterials*, 22(8), 799-806.
- [25] Marra, S.P., Ramesh, K.T., and Douglas, A.S., **2001**, *Mat. Sci. Eng. C-Bio. S.*, 14(1-2), 25-34.
- [26] Anseth, K.S., Bowman, C.N., and BrannonPeppas, L., **1996**, *Biomaterials*, 17(17), 1647-1657.
- [27] Yasuda, H., Lamaze, C.E., and Peterlin, A., **1971**, *J. Polym. Sci. A2*, 9(6),pp. 1117-1131.
- [28] Refojo, M.F., **1965**, *J. Appl. Polym. Sci.*, 9(10), pp. 3417-3426.
- [29] Chiarelli, P., Basser, P.J., Derossi, D., and Goldstein, S., **1992**, *Biorheology*, 29, pp. 383-398.
- [30] LeRoux, M.A. and Setton, L.A., **2002**, *J. Biomech. Eng.-Trans. ASME*, 124(3), pp. 315-321.
- [31] Hoffman, A.S., **2002**, *Adv. Drug Deliver. Rev.*,54(1), pp. 3-12.
- [32] Manetti, C., Casciani, L., and Pescosolido, N., **2002**, *Polymer*, 43(1), pp. 87-92.